Title

Exposure to a Histone Deacetylase Inhibitor Has Detrimental Effects on Human Lymphocyte Viability and Function

Journal

Cancer Immunology Research, 2(5)

ISSN

2326-6066

Authors

Wong, Deborah JL
Rao, Amol
Avramis, Earl
et al.

Publication Date

2014-05-01

DOI

10.1158/2326-6066.cir-13-0188

Peer reviewed

Published in final edited form as:
Cancer Immunol Res. 2014 May ; 2(5): 459–468. doi:10.1158/2326-6066.CIR-13-0188.

Exposure to a histone deacetylase inhibitor has detrimental effects on human lymphocyte viability and function

Deborah J.L. Wong[1], **Amol Rao**[1], **Earl Avramis**[1], **Douglas R. Matsunaga**[1], **Kimberly M. Komatsubara**[2], **Mohammad S. Atefi**[1], **Helena Escuin-Ordinas**[1], **Thinle Chodon**[3], **Richard C. Koya**[3], **Antoni Ribas**[1,4,5], and **Begoña Comin-Anduix**[4,5,*]

[1]Department of Medicine, Division of Hematology-Oncology, University of California Los Angeles, Los Angeles, California (UCLA)

[2]Department of Medicine. Stanford Hospital and Clinics. Stanford, CA

[3]Department of Immunology. Roswell Park Cancer Institute, Buffalo, New York

[4]Department of Surgical-Oncology, University of California Los Angeles, Los Angeles, UCLA

[5]Jonsson Comprehensive Cancer Center at UCLA

Abstract

Histone deacetylase inhibitors (HDACi) have been reported to increase tumor antigen expression, and have been successfully tested as adjuvants for melanoma immunotherapy in mouse models. In this work, we tested the effects of a pan-HDACi on human lymphocytes and melanoma cell lines. Effects of the pan-HDACi panobinostat (LBH589) on cell viability, cell cycle, apoptosis and DNA damage were determined in peripheral blood mononuclear cells (PBMC) from two healthy donor (HD), thirteen patients with metastatic melanoma (MD), two bone marrow samples from patients with different malignances, and twelve human melanoma cell lines. Intracellular signaling in lymphocytes, with or without cytokine stimulation, was analyzed by phospho-flow cytometry in one of each type. The 50% inhibition concentration (IC_{50}) in PBMC was < 20 nM compared to > 600 nM in melanoma cell lines; > 40% apoptotic cell death in PBMC versus < 10% in melanoma cell lines was seen at the same concentration. Phospho-histone variant H2A.X (pH2A.X) increased 2-fold in HD PBMC at 1 nM, while the same effect in the melanoma cell line M229 required 10nM. pH2A.X was inhibited slightly in the PBMC of 3 MD at 1 nM and in the melanoma cell line M370 at 10 nM. Panobinostat inhibited phospho-STAT1/3/5/6, -p38, -ERK, -p53, -cyclin D3, and -histone H3 in flow cytometry-gated HD B- and T-cells, while it induced up to six-fold activation in MD and bone marrow samples. In human lymphocytes, panobinostat alters key lymphocyte activation signaling pathways and is cytotoxic at concentrations much lower than that required for melanoma antitumor activity, resulting in an adverse therapeutic window.

[*]**Corresponding Author**: Begoña Comin-Anduix, Division of Surgery, 54–140 CHS, UCLA Medical Center, 10833 Le Conte Avenue, Los Angeles, CA 90095-1782, Jonsson Comprehensive Cancer Center. bcomin@mednet.ucla.edu, Telephone: 310-267-2211; Fax: 310-825-4437.

Conflict of interest: The authors have no conflicts of interest to disclose.

Keywords

human melanoma cells; Human lymphocytes; HDACi

Introduction

Histone deacetylases (HDAC) are enzymes that play key regulatory roles in gene expression and cellular differentiation. HDAC functions include the removal of acetyl groups from transcription factors (e.g. p53) (1) and signal transduction proteins (e.g. STAT3) (1), and the acetylation of the molecular chaperone Hsp90 (2) and alpha-tubulin (2, 3). Given the crucial role of HDAC as cellular epigenetic modifiers, inhibitors of HDAC proteins (HDACi) have been evaluated for clinical application as anti-cancer therapies. There are eighteen HDAC enzymes in 4 subclasses (4): classes I, II, and IV are zinc-finger metalloproteinase; class III are NAD^+-dependent proteins.

HDACi inhibit the zinc-finger metalloproteinase HDAC by binding the zinc-finger domain in the catalytic site. The pan-HDACi vorinostat (Zolinza) and the class I HDACi romidepsin (Istodax) were approved by the US FDA for the treatment of cutaneous T-cell lymphoma in 2006 and in 2009, respectively (5, 6). Several other HDACi, including the pan-HDACi panobinostat (LBH589), are being investigated in clinical trials. Among the hydroxamic acid HDACi, panobinostat has the most potent inhibitory activity (7). Panobinostat is a second generation HDACi; it has potent antitumor activity *in vitro* in T-cell lymphoma, Hodgkin's lymphoma, and chronic myelogenous leukemia. In Phase I and II clinical trials panobinostat has demonstrated the most efficacy in refractory cutaneous T-cell lymphoma, although studies are still ongoing in multiple myeloma, non-Hodgkin's lymphoma, and gastric cancer (www.clinicaltrials.gov). Similar to other HDACi, the most common side effects include nausea, diarrhea, fatigue, thrombocytopenia and other cytopenias, all of which typically are managed easily (8). Panobinostat inhibits the growth of pancreatic, breast, prostate and colon cancer cell lines, however, clinical data for panobinostat alone in solid tumors have been less robust than those for hematologic malignancies (6).

Several ongoing clinical trials are evaluating the safety and efficacy of adoptive cell therapy (ACT) for melanoma. In some of these studies, genetically engineered T-cells expressing tumor-specific T-cell receptors (TCR) are infused into patients after conditioning chemotherapy and lymphodepletion followed by the administration of interleukin-2 (IL2) to stimulate T cell proliferation *in vivo*. ACT can result in objective and durable responses in humans however, the response rates tend to be not durable (9, 10). Therefore, agents that can be used safely as adjuncts to ACT are of interest (11).

To this end, several published reports have demonstrated that HDACi sensitized cancer cells to immunotherapy. HDACi upregulate genes important in apoptosis (12–16), and increase the expression of proteins involved in antigen processing and presentation (17–19), of tumor antigens, and of ligands that can be recognized by NK cells (19–22). In mouse models of solid tumors, the antitumor effect of HDACi can be augmented by manipulating the immune system. Combining vorinostat or panobinostat with antibodies to CD40, which stimulates antigen presenting cells, or to CD137, which co-stimulates cytotoxic T-lymphocytes (CTL),

led to enhanced tumor regression in mouse models of breast, renal and colon carcinomas (23). Similar findings have been shown in mouse models of melanoma: treatment of B16 murine melanoma with both the pan-HDACi LAQ824 (dacinostat) and ACT of pmel-1 T-cells specific for the gp100 melanoma antigen resulted in increased antitumor activity (24). The ability of LAQ824 to augment the effects of immune therapy was also demonstrated in a prophylactic prime-boost vaccination mouse model of melanoma using the melanoma antigen tyrosinase-related protein-2 (25). The class I HDACi depsipeptide (romidepsin) increased the expression of the gp100/pmel melanoma antigen and sensitized B16 melanoma cells to Fas ligand *in vitro*, resulted in enhanced antitumor activity in the ACT study (26).

While these mouse data are promising, HDACi have been shown to enhance the effects of regulatory T cells (Treg) and inhibit cell cycle progression of lymphocytes (27–31). Furthermore, Song and colleagues have demonstrated that treatment of myeloid dendritic cells (DC) from healthy donors with panobinostat impaired DC functions, decreased the expression of surface molecules associated with DC maturation, and reduced antigen presentation, and T-cell co-stimulation (32). Therefore, it is unclear whether HDACi can be safe and effective as adjuncts to immunotherapy. To further evaluate the potential of HDACi in combination with immunotherapy, we studied the effects of panobinostat in human melanoma cell lines and human lymphocytes on growth inhibition, cell cycle progression, and effects on MAPK and PI3K signaling by phosphos-flow analysis. In this study we focus on the effects of panobinostat given its *in vitro* potency so that the effects in human cells could be directly compared with the results published by Song and colleagues (32).

Materials and Methods

Reagents and Cell Lines

Panobinostat (LBH589) was obtained from Novartis (Basel, Switzerland) and reconstituted in dimethyl sulfoxide (DMSO) to a final stock concentration of 10mM. Peripheral blood mononuclear cells (PBMC) were obtained by leukapheresis from two healthy subject (HD) under UCLA IRB #04-07-063 and 12 patients with metastatic melanoma (MD) not on active therapy under UCLA IRB 10-000870, bone marrow from a patient with multiple myeloma (BM-1) or a patient with breast cancer (BM-2) obtained under UCLA IRB 08-08-062, or PBMC from a healthy donor were transduced twice in retronectin-coated plates with a retrovirus expressing a high-affinity Melan-A/MART-1 TCR (33). PBMC were cultured in RPMI 1640 with L-glutamine (Mediatech Inc., Manassas, VA) containing 5% human AB serum (Omega Scientific, Tarzana, CA) at a density of 1 million cells/mL. Proliferating PBMC were cultured at a density of 0.7 million cells/mL in 300 IU/mL of IL2 (Novartis) with 50 ng/mL of anti-human CD3 antibody OKT3 (eBioscience, San Diego, CA), added for the first 48 hours of culture only. The human melanoma cell lines M202, M229, M233, M249, M263, M285, M308, M370, M376, M395, M408, and M417 were established from patient biopsies under UCLA IRB #02–08-067 as described (34, 35). Melanoma cells were cultured in RPMI 1640 with L-glutamine containing 10% fetal bovine serum (FBS, Omega Scientific) and 1% penicillin, streptomycin and fungizone (PSF, Omega Scientific). All cell lines were negative for mycoplasma (MycoAlert PLUS Mycoplasma Detection kit; Lonza Ltd, Basel, Switzerland).

Cell viability assays

6 PBMC and 2 melanoma cell lines were treated in triplicate with 0, 0.1nM, 1nM, 10 nM, 100 nM, 1 μM, 10 μM and 100μM panobinostat, or DMSO as vehicle control (VC), for 72 hours. Viability was analyzed using an ATP-based luminescent cell proliferation assay kit following the manufacturer's instructions (CellTiter-Glo Luminescent Cell Viability Assay; Promega, Madison, WI). Data were analyzed using Microsoft Excel and the 50% inhibitory concentration (IC_{50}) was then calculated using GraphPad Prism.

Cell-cycle analysis and assessment of apoptosis by flow cytometry

6 PBMC and 2 melanoma cell lines were incubated for 72 hours with 0.1nM, 1 nM, 10 nM, 100 nM, 1 μM, 10 μM of panobinostat, DMSO, and 1 μM of staurosporine as a positive control, fixed (BD Cytofix/Cytoperm; BD Biosciences, San Jose, CA), washed (BD Perm/Wash Buffer), and stained for cleaved poly[ADP-ribose]polymerase (PARP) (clone F21-852; BD Biosciences). After incubation, cells were washed and resuspended in a solution of 2 μM of 40,6-diamidino-2-phenylindole (DAPI), 0.001% nonaderent-40, and 1% bovine serum albumin in Dulbecco-PBS (Sigma-Aldrich, St. Louis, MO). 12,000 cellular events in G0-G1 per sample were acquired for analysis. Data were analyzed using FlowJo (Tree Star, Inc, Ashland, OR).

Assessment of DNA damage by flow cytometry

Phosphorylation of histone variant H2A.X (pH2A.X) as a marker of DNA damage was determined using the FlowCellect Multi-Color DNA Damage Response Kit (Millipore Billerica, MA). 6 PBMC and 2 melanoma cell lines were treated with 0.1nM, 1 nM, 10 nM, 100 nM, 1 μM, 10 μM of panobinostat or DMSO as VC, fixed, permeabilized, washed using the buffers provided, and then stained with pHistone-H2A.X-PerCP (Millipore) per manufacturer's specifications. Events were collected by flow cytometry and data analysis was carried out using Cytobank (www.cytobank.org).

Phospho-proteomic platform at a single cell level

Phosphorylated intracellular signaling molecules at single cell level were detected as described (33). Briefly, 2 PBMC samples and a bone marrow sample from a patient with multiple myeloma (BM-1) were cultured in 0.1nM, 1 nM, 10 nM, 100 nM, and 1 μM panobinostat for 24 hours and then stimulated for 15 minutes with 10,000 IU/mL IFN-α or 400 IU/mL of IL2. After stimulation, cells were surface-stained, then fixed with formaldehyde to a final concentration of 1.6%, and permeabilized using methanol (90%). Fluorescent barcoding of PBMC was carried out with a combination of 0, 3 or 8 μg/mL of Ax350-NHS and 0, 3 or 8 μg/mL of Ax750-NHS to allow the simultaneous analysis of 6 different populations in 1 sample. After two washes, barcoded samples were incubated for 30 minutes with cocktails of antibodies to simultaneously stain intracellular proteins. In total, 5 different antibody cocktails were used per condition (Supplemental Table 1). All antibodies were used at saturating concentrations. Flow Cytometric compensation was carried out using anti-mouse Igκ/Negative Control FBS compensation particles (BD Biosciences). 100,000 to 300,000 lymphocyte events were collected by flow cytometry and analyzed using Cytobank (www.cytobank.org).

Statistical analysis

Due to the small size of the population, statistical analyses are essentially descriptive.

Each experiment was performed at a minimum in triplicate independent studies, with each sample in duplicate or triplicate for each experiment. Descriptive data analysis was performed with Microsoft Excel and GraphPad Prism (v4) and paired t-test was applied. All flow cytometry experiments were carried out using an LSRII (BD Biosciences), using biexponential axis.

Results

Effects of panobinostat on melanoma cell lines and human PBMC

In order to determine the susceptibility of human cells to panobinostat, twelve melanoma cell lines, resting PBMC, and activated PBMC from multiple donor sources were treated with increasing concentrations of panobinostat for 72 hours and the 50% inhibitory concentration (IC_{50}) was determined. In addition to PBMC from melanoma subjects, specimens from healthy subjects or subjects with non-melanoma solid tumor (breast cancer) and hematologic malignancy (multiple myeloma) were chosen to determine if the source of lymphocytes would impact the results. As shown in Figure 1, the human PBMC and melanoma cell lines tested fell into 3 categories with respect to sensitivity to panobinostat: IC_{50} of 20 nM or less (defined as sensitive), IC_{50} of 21–50 nM (intermediately sensitive), and IC_{50} of greater than 50 nM (resistant), consistent with previous published reports (7). Thirteen of fifteen resting PBMC specimens (both, HD and MD) were sensitive to panobinostat; MD8 was intermediately sensitive with an IC_{50} of 26 nM. Twelve of seventeen anti-CD3 and IL2-activated PBMC were sensitive, with an additional three activated PBMC samples showing intermediate sensitivity. Of the ten of eleven patient samples for which both resting and activated PBMC were evaluated, the activated PBMC were generally less sensitive to panobinostat. However, with the exception of the activated MD7 (IC_{50} 22.4 nM), all ten of these activated samples remained sensitive to panobinostat. For MD9, the IC_{50} of the resting PBMC was less than two times greater than that of the activated PBMC, though both samples were highly sensitive to panobinostat (16 and 12 nM, respectively). To evaluate the potential utility of panobinostat for immunotherapy, we evaluated the effects of panobinostat on PBMC from a healthy donor (T-HD1) and from a patient with metastatic melanoma (T-MD5) both PBMC samples had been transduced to express the TCR for melanoma antigen MART-1. While T-MD5 was sensitive with an IC_{50} of 14 nM, the IC_{50} of T-HD1 was 80 nM. The bone marrow from a patient with multiple myeloma (BM-1) was resistant to panobinostat with an IC_{50} of 90nM. In all, 24 of 30 PBMC samples tested were sensitive to panobinostat.

Of the twelve melanoma cell lines studied, seven had mutations at $BRAF^{V600E}$, two had mutations at $NRAS^{Q61}$, one had both $BRAF^{V600E}$/$NRAS^{Q61K}$ mutations, and one was wild-type for the *BRAF* and *NRAS* genes. Table 1 lists the characteristics of the 12 melanoma cell lines and their sensitivity to vemurafenib, an FDA-approved targeted therapy for metastatic melanoma (34–36). In contrast to results for PBMC, only 2 of 12 human melanoma cells were sensitive to panobinostat, including M308, a $BRAF^{V600E}$-mutant melanoma cell line

highly resistant to vemurafenib. Four melanoma cell lines had intermediate sensitivity to panobinostat while the remaining six were resistant to panobinostat, including three with IC_{50} of greater than 100 nM (IC_{50} 55–125nM). Neither the BRAF wild-type (M285) nor the NRAS-mutated melanoma cell lines (M202, M408 and M376) were sensitive to panobinostat.

Effects of panobinostat on cell-cycle progression and apoptosis

Cell-cycle analysis by flow cytometry was performed to determine the effects of panobinostat in melanoma or activated PBMC. Four sensitive (HD1, MD1, MD2, MD3), one intermediately sensitive (MD4) and three resistant samples (T-HD1, M229, and M370) were exposed to 0–10 μM panobinostat for 24 hours and then analyzed by DAPI staining combined with intracellular staining for cleaved PARP. As shown in Figure 2, panobinostat increased the sub-G0 population of cells for all samples, though the most profound effect was seen in the sensitive cells HD1, MD1, MD2, MD3 and MD4. Furthermore, cleaved PARP staining increased with panobinostat treatment. Indeed, in all lymphocyte samples, nearly all cells in sub-G0, G0/G1, and G2/M were positive for cleaved PARP (Figure 2A). While the G0/G1 population of cells increased at 1 nM for MD1 and MD2 lymphocytes, no other statistically significant trends in the G0/G1, G2/M or S cell populations were seen with increasing panobinostat concentration. Instead, with the exception of M370, a dramatic cytotoxic effect was observed for all samples (Figure 2B). Panobinostat induced 30% or greater apoptotic cell death demonstrated by cleaved PARP in PBMC samples, while it was about 10% in M229 and 8% in M370 at 100 nM. Only at 10 μM was cleaved PARP about 30% for M229 while approximately 10% cleaved PARP was observed for M370 at this this concentration (Figure 2C). We stained for phosphorylated histone variant, H2A.X (pH2A.X) by flow cytometry as a marker of DNA damage (37). With the exception of M370, there was an up to 3-fold increase in pH2A.X in all PBMC at 10 μM (Figure 3). For M370, pH2A.X increased by less than 2-fold, even at 10 μM. These studies support the notion that panobinostat has greater cytostatic and cytotoxic effects on human T cells than on melanoma cells.

Single cell phospho-proteomic analysis of lymphocytes after exposure to panobinostat

Using phospho-flow, we studied the effects of panobinostat on lymphocyte signaling proteins, including key MAPK and PI3K/AKT signaling proteins and those downstream of the TCR, B-cell receptor (BCR), and cytokine receptors in one sample each of healthy, melanoma donor, and bone marrow specimens. Two of them were sensitive (HD1 [IC_{50} < 10 nmol/l] and MD2 [IC_{50} > 10 nmol/l] and one resistant (BM-1, [IC_{50} < 50 nmol/l]) to panobinostat. Given that IFN-α or IL-2 are key lymphocyte signaling cytokines and are often used clinically to treat advanced melanoma, activated lymphocytes stimulated with IFN-α or IL-2 were studied after 24 hour exposure to panobinostat and stained for surface and intracellular proteins. Figure 4 shows the gating strategy used for these analyses.

Panobinostat slightly inhibited the phosphorylation of STAT5, ERK1/2 and H3 in flow-gated T-cells from a healthy donor at concentrations of 10 nM and 100 nM. At higher concentrations, there was a slight increase in these phosphoproteins. In contrast, CD8 and CD4 T cells from the patient with metastatic melanoma (MD2) demonstrated a uniform

increase in all intracellular proteins with increasing concentrations of panobinostat. CD8 cells from MD2 had an approximately 4-fold increase in pSTAT1, pSTAT3, pSTAT5, pAKT, pERK1/2, pP38, pP53, CyD3, and pH3. Similarly, for MD2 CD4 T cells, pSTAT1, pSTAT3, pSTAT6, pAKT, pERK1/2, CyD3 and pH3 were increased by 4-fold compared to controls. pSTAT5, pP38 and pP53 were increased almost 8-fold in MD2 CD4 cells activated with IL2 or vehicle control. Treatment with IFN blunted the effect of panobinostat as the levels of intracellular phosphoproteins were slightly less than that seen in vehicle control using the same concentration of panobinostat. Panobinostat treatment of CD8 and CD4 cells from the bone marrow of a patient with multiple myeloma (BM-1) increased pSTAT1, pSTAT5, pSTAT6, pP38, pP53 and CyD3 in vehicle control cells, while it induced a 6-fold increase in pH3. In these cells, treatment with IFN or IL2 blunted this effect. These trends for each patient sample were consistent for CD20 cells (Figure 5 and data not shown). These data indicate that panobinostat activates the MAPK and PI3K/AKT signaling in human lymphocytes, especially those from melanoma and myeloma patients.

Discussion

In this *in vitro* study the majority of the human lymphocytes were highly susceptible to treatment with panobinostat at 20nM or less, which were doses lower than that required to inhibit the melanoma cell lines. Most lymphocytes, resting or proliferating, are susceptible to panobinostat inhibition whether they were derived from the peripheral blood or the bone marrow, from healthy subjects or patients with melanoma or multiple myeloma. Only a minority of the 12 melanoma cell lines tested were sensitive to panobinostat. Growth inhibition of lymphocytes was mediated primarily via increased apoptosis demonstrated by cleaved PARP and in the sub-G0 population. Increased DNA damage was induced in some lymphocyte cultures. Panobinostat upregulated MAPK and PI3K/AKT phosphoproteins by 4 to 8 fold compared to controls. This induction was even more pronounced in human lymphocytes from patients with myeloma or melanoma compared to a healthy donor.

This is the first report evaluating the inhibitory effect of panobinostat in a large panel of melanoma cell lines, which included several BRAF-mutant and wild-type melanoma cell lines inherently resistant to vemurafenib. These data are consistent with prior reports demonstrating that HDACi generally have only a modest inhibitory effect in solid tumors compared to hematologic malignancies (7, 38, 39). The melanoma cell lines tested in our study were derived from cutaneous melanoma, and not from uveal melanoma. A report had suggested that uveal melanoma cell lines may be more sensitive to panobinostat with IC_{50} of 60 nM or lower (40). This growth inhibition may be mediated, at least in part, by the suppression of the expression of microphthalmia-associated transcription factor (MITF) as the treatment with panobinostat resulted in a decrease in MITF-M proteins (41). Therefore, additional studies to evaluate the clinical applicability of panobinostat in uveal melanoma may be worthwhile.

The multicolor flow cytometry used in this study for single-cell phospho-proteomic analysis provides a powerful tool to gain insight into the effects of panobinostat on signaling networks within individual PBMC subpopulations (42). In addition to qualitative analysis, the phosphor-flow technique affords a highly reproducible, quantitative evaluation of the

changes in intracellular phosphoproteins at the level of individual lymphocytes (33, 43). In contrast to treatment with vemurafenib, which resulted in little change in phosphoproteins or lymphocyte function at concentrations below 50 μM (33), panobinostat upregulated proteins in key signaling pathways in all cells tested. Therefore, we hypothesize that panobinostat exerts its toxic effect on lymphocytes by upregulating signaling molecules that lead to decreased function and increased cytotoxicity.

In mouse models of melanoma, HDACi increased the expression of proteins involved in antigen presentation and processing (44). Despite promising mouse data demonstrating synergy of HDACi with anti-CD40 and anti-CD137 (23) or in combination with ACT therapy (24, 25), our data with panobinostat in human lymphocytes should temper enthusiasm for combining HDACi with immunotherapy given the cytotoxic effect of panobinostat on lymphocytes at concentrations lower than that required to inhibit most melanoma cell lines. Consistent with this, panobinostat had a detrimental effect on human dendritic cell (DC) viability and function (31). Panobinostat also decreased the expression of T-cell activating co-stimulatory receptor CD40, DC- and T-cell-activating receptor CD83 (23), and antigen presenting molecules HLA-A/B/C (31). Our data in human lymphocytes are not surprising given that pan-HDAC inhibitors have clinical application in the treatment of T-cell malignancies and are under active investigation in early-phase clinical trials for the treatment of other hematologic malignancies such as multiple myeloma, Hodgkin's lymphoma, and chronic myelogenous leukemia, and as immunomodulatory agents in inflammatory disorders such as rheumatoid arthritis. Due to the deleterious effects of panobinostat on human lymphocytes, we conclude that it is likely not a suitable adjunct therapy after ACT. Instead, one potential application could be as an adjunct for lymphodepletion prior to ACT or as useful immunosuppressive agent, though additional investigations into this potential clinical application should be undertaken. Alternatively, development of panobinostat as a local therapy via intratumoral injections or delivered via nanoparticles to minimize systemic toxicity may also be a consideration.

One strategy to augment responses to immunotherapy is combination therapy with agents that increase antigen presentation to T cells. Histone deacetylase inhibitors have been reported to increase melanosomal antigen expression and improve combinatorial effect with immunotherapy in mouse models. However, exposure to a pan-HDACi resulted in both cytostatic and cytotoxic effects on human lymphocytes *in vitro* as it altered key lymphocyte signaling networks. These human *in vitro* data may argue against the use of panobinostat, a hydroxamic acid HDACi, in combination with immunotherapies in the clinic for melanoma patients.

Supplementary Material

Refer to Web version on PubMed Central for supplementary material.

Acknowledgments

This work was funded by NIH grants 2U54 CA151819, R01 CA170689 and PO1 CA168585, The Seaver Institute, the Dr. Robert Vigen Memorial Fund, the Wesley Coyle Memorial Fund, the Garcia-Corsini Family Fund, the Louise Belley and Richard Schnarr Fund, the Bila Alon Hacker Memorial Fund, the Fred L. Hartley Family

Foundation, the Ruby Family Foundation, the Jonsson Cancer Center Foundation, and the Caltech-UCLA Joint Center for Translational Medicine (to A.R.). R.C.K. and H.E-O. were supported by the V Foundation-Gil Nickel Family Endowed Fellowship in Melanoma Research. Flow cytometry was performed in the UCLA Jonsson Comprehensive Cancer Center (JCCC) and Center for AIDS Research Flow Cytometry Core Facility that is supported by National Institutes of Health awards CA-16042 and AI-28697, and by the JCCC, the UCLA AIDS Institute, and the David Geffen School of Medicine at UCLA.

References

1. Gu W, Roeder RG. Activation of p53 sequence-specific DNA binding by acetylation of the p53 C-terminal domain. Cell. 1997; 90(4):595–606. [PubMed: 9288740]
2. Kovacs JJ, Murphy PJ, Gaillard S, Zhao X, Wu JT, Nicchitta CV, et al. HDAC6 regulates Hsp90 acetylation and chaperone-dependent activation of glucocorticoid receptor. Molecular cell. 2005; 18(5):601–607. [PubMed: 15916966]
3. Hubbert C, Guardiola A, Shao R, Kawaguchi Y, Ito A, Nixon A, et al. HDAC6 is a microtubule-associated deacetylase. Nature. 2002; 417(6887):455–458. [PubMed: 12024216]
4. Woan KV, Sahakian E, Sotomayor EM, Seto E, Villagra A. Modulation of antigen-presenting cells by HDAC inhibitors: implications in autoimmunity and cancer. Immunology and cell biology. 2012; 90(1):55–65. [PubMed: 22105512]
5. Wilcox RA. Cutaneous T-cell lymphoma: 2011 update on diagnosis, risk-stratification, and management. American journal of hematology. 2011; 86(11):928–948. [PubMed: 21990092]
6. Robey RW, Chakraborty AR, Basseville A, Luchenko V, Bahr J, Zhan Z, et al. Histone deacetylase inhibitors: emerging mechanisms of resistance. Molecular pharmaceutics. 2011; 8(6):2021–2031. [PubMed: 21899343]
7. Atadja P. Development of the pan-DAC inhibitor panobinostat (LBH589): successes and challenges. Cancer letters. 2009; 280(2):233–241. [PubMed: 19344997]
8. DeAngelo DJ, Spencer A, Bhalla KN, Prince HM, Fischer T, Kindler T, et al. Phase Ia/II, two-arm, open-label, dose-escalation study of oral panobinostat administered via two dosing schedules in patients with advanced hematologic malignancies. Leukemia. 2013; 27(8):1628–1636. [PubMed: 23385375]
9. Rosenberg SA, Restifo NP, Yang JC, Morgan RA, Dudley ME. Adoptive cell transfer: a clinical path to effective cancer immunotherapy. Nat Rev Cancer. 2008; 8(4):299–308. [PubMed: 18354418]
10. Rosenberg SA, Yang JC, Sherry RM, Kammula US, Hughes MS, Phan GQ, et al. Durable complete responses in heavily pretreated patients with metastatic melanoma using T-cell transfer immunotherapy. Clinical cancer research : an official journal of the American Association for Cancer Research. 2011; 17(13):4550–4557. [PubMed: 21498393]
11. Ribas A, Wolchok JD. Combining cancer immunotherapy and targeted therapy. Current opinion in immunology. 2013; 25(2):291–296. [PubMed: 23561594]
12. Nebbioso A, Clarke N, Voltz E, Germain E, Ambrosino C, Bontempo P, et al. Tumor-selective action of HDAC inhibitors involves TRAIL induction in acute myeloid leukemia cells. Nat Med. 2005; 11(1):77–84. [PubMed: 15619633]
13. Peart MJ, Smyth GK, van Laar RK, Bowtell DD, Richon VM, Marks PA, et al. Identification and functional significance of genes regulated by structurally different histone deacetylase inhibitors. Proc Natl Acad Sci U S A. 2005; 102(10):3697–3702. [PubMed: 15738394]
14. Zhang XD, Gillespie SK, Borrow JM, Hersey P. The histone deacetylase inhibitor suberic bishydroxamate: a potential sensitizer of melanoma to TNF-related apoptosis-inducing ligand (TRAIL) induced apoptosis. Biochem Pharmacol. 2003; 66(8):1537–1545. [PubMed: 14555232]
15. Zhang XD, Gillespie SK, Borrow JM, Hersey P. The histone deacetylase inhibitor suberic bishydroxamate regulates the expression of multiple apoptotic mediators and induces mitochondria-dependent apoptosis of melanoma cells. Mol Cancer Ther. 2004; 3(4):425–435. [PubMed: 15078986]
16. Insinga A, Monestiroli S, Ronzoni S, Gelmetti V, Marchesi F, Viale A, et al. Inhibitors of histone deacetylases induce tumor-selective apoptosis through activation of the death receptor pathway. Nat Med. 2005; 11(1):71–76. [PubMed: 15619634]

17. Maeda T, Towatari M, Kosugi H, Saito H. Up-regulation of costimulatory/adhesion molecules by histone deacetylase inhibitors in acute myeloid leukemia cells. Blood. 2000; 96(12):3847–3856. [PubMed: 11090069]

18. Magner WJ, Kazim AL, Stewart C, Romano MA, Catalano G, Grande C, et al. Activation of MHC class I, II, and CD40 gene expression by histone deacetylase inhibitors. J Immunol. 2000; 165(12): 7017–7024. [PubMed: 11120829]

19. Setiadi AF, Omilusik K, David MD, Seipp RP, Hartikainen J, Gopaul R, et al. Epigenetic enhancement of antigen processing and presentation promotes immune recognition of tumors. Cancer Res. 2008; 68(23):9601–9607. [PubMed: 19047136]

20. Armeanu S, Bitzer M, Lauer UM, Venturelli S, Pathil A, Krusch M, et al. Natural killer cell-mediated lysis of hepatoma cells via specific induction of NKG2D ligands by the histone deacetylase inhibitor sodium valproate. Cancer Res. 2005; 65(14):6321–6329. [PubMed: 16024634]

21. Skov S, Pedersen MT, Andresen L, Straten PT, Woetmann A, Odum N. Cancer cells become susceptible to natural killer cell killing after exposure to histone deacetylase inhibitors due to glycogen synthase kinase-3-dependent expression of MHC class I-related chain A and B. Cancer Res. 2005; 65(23):11136–11145. [PubMed: 16322264]

22. Konkankit VV, Kim W, Koya RC, Eskin A, Dam MA, Nelson S, et al. Decitabine immunosensitizes human gliomas to NY-ESO-1 specific T lymphocyte targeting through the Fas/Fas ligand pathway. Journal of translational medicine. 2011; 9:192. [PubMed: 22060015]

23. Christiansen AJ, West A, Banks KM, Haynes NM, Teng MW, Smyth MJ, et al. Eradication of solid tumors using histone deacetylase inhibitors combined with immune-stimulating antibodies. Proceedings of the National Academy of Sciences of the United States of America. 2011; 108(10): 4141–4146. [PubMed: 21368108]

24. Vo DD, Donahue TR, De La Rocha P, Begley JL, Yang M-Y, Kharazi P, et al. A Histone Deacetylase Inhibitor (HDACi) Sensitizes B16 Melanoma to Adoptive Transfer (AT) Immunotherapy. Proc. International Society of Biological Therapy for Cancer. 2006 (abstract).

25. Vo DD, Prins RM, Begley JL, Donahue TR, Morris LF, Bruhn KW, et al. Enhanced Antitumor Activity Induced by Adoptive T-Cell Transfer and Adjunctive Use of the Histone Deacetylase Inhibitor LAQ824. Cancer Res. 2009

26. Murakami T, Sato A, Chun NA, Hara M, Naito Y, Kobayashi Y, et al. Transcriptional modulation using HDACi depsipeptide promotes immune cell-mediated tumor destruction of murine B16 melanoma. The Journal of investigative dermatology. 2008; 128(6):1506–1516. [PubMed: 18185535]

27. Brogdon JL, Xu Y, Szabo SJ, An S, Buxton F, Cohen D, et al. Histone deacetylase activities are required for innate immune cell control of Th1 but not Th2 effector cell function. Blood. 2007; 109(3):1123–1130. [PubMed: 17008546]

28. Kato Y, Yoshimura K, Shin T, Verheul H, Hammers H, Sanni TB, et al. Synergistic in vivo antitumor effect of the histone deacetylase inhibitor MS-275 in combination with interleukin 2 in a murine model of renal cell carcinoma. Clin Cancer Res. 2007; 13(15 Pt 1):4538–4546. [PubMed: 17671140]

29. Reilly CM, Mishra N, Miller JM, Joshi D, Ruiz P, Richon VM, et al. Modulation of renal disease in MRL/lpr mice by suberoylanilide hydroxamic acid. J Immunol. 2004; 173(6):4171–4178. [PubMed: 15356168]

30. Johnson J, Pahuja A, Graham M, Hering B, Hancock WW, Bansal-Pakala P. Effects of histone deacetylase inhibitor SAHA on effector and FOXP3+regulatory T cells in rhesus macaques. Transplantation proceedings. 2008; 40(2):459–461. [PubMed: 18374101]

31. Wang L, de Zoeten EF, Greene MI, Hancock WW. Immunomodulatory effects of deacetylase inhibitors: therapeutic targeting of FOXP3+ regulatory T cells. Nature reviews. Drug discovery. 2009; 8(12):969–981.

32. Song W, Tai YT, Tian Z, Hideshima T, Chauhan D, Nanjappa P, et al. HDAC inhibition by LBH589 affects the phenotype and function of human myeloid dendritic cells. Leukemia. 2011; 25(1):161–168. [PubMed: 21102427]

33. Comin-Anduix B, Chodon T, Sazegar H, Matsunaga D, Mock S, Jalil J, et al. The oncogenic BRAF kinase inhibitor PLX4032/RG7204 does not affect the viability or function of human lymphocytes across a wide range of concentrations. Clin Cancer Res. 2010; 16(24):6040–6048. [PubMed: 21169256]
34. Atefi M, von Euw E, Attar N, Ng C, Chu C, Guo D, et al. Reversing melanoma cross-resistance to BRAF and MEK inhibitors by co-targeting the AKT/mTOR pathway. PloS one. 2011; 6(12):e28973. [PubMed: 22194965]
35. Sondergaard JN, Nazarian R, Wang Q, Guo D, Hsueh T, Mok S, et al. Differential sensitivity of melanoma cell lines with BRAFV600E mutation to the specific raf inhibitor PLX4032. J Transl Med. 2010; 8(1):39. [PubMed: 20406486]
36. von Euw E, Atefi M, Attar N, Chu C, Zachariah S, Burgess BL, et al. Antitumor effects of the investigational selective MEK inhibitor TAK733 against cutaneous and uveal melanoma cell lines. Molecular cancer. 2012; 11(1):22. [PubMed: 22515704]
37. Pettazzoni P, Pizzimenti S, Toaldo C, Sotomayor P, Tagliavacca L, Liu S, et al. Induction of cell cycle arrest and DNA damage by the HDAC inhibitor panobinostat (LBH589) and the lipid peroxidation end product 4-hydroxynonenal in prostate cancer cells. Free radical biology & medicine. 2011; 50(2):313–322. [PubMed: 21078383]
38. Crisanti MC, Wallace AF, Kapoor V, Vandermeers F, Dowling ML, Pereira LP, et al. The HDAC inhibitor panobinostat (LBH589) inhibits mesothelioma and lung cancer cells in vitro and in vivo with particular efficacy for small cell lung cancer. Molecular cancer therapeutics. 2009; 8(8): 2221–2231. [PubMed: 19671764]
39. Tate CR, Rhodes LV, Segar HC, Driver JL, Pounder FN, Burow ME, et al. Targeting triple-negative breast cancer cells with the histone deacetylase inhibitor panobinostat. Breast cancer research : BCR. 2012; 14(3):R79. [PubMed: 22613095]
40. Landreville S, Agapova OA, Matatall KA, Kneass ZT, Onken MD, Lee RS, et al. Histone deacetylase inhibitors induce growth arrest and differentiation in uveal melanoma. Clinical cancer research : an official journal of the American Association for Cancer Research. 2012; 18(2):408–416. [PubMed: 22038994]
41. Yokoyama S, Feige E, Poling LL, Levy C, Widlund HR, Khaled M, et al. Pharmacologic suppression of MITF expression via HDAC inhibitors in the melanocyte lineage. Pigment cell & melanoma research. 2008; 21(4):457–463. [PubMed: 18627530]
42. Krutzik PO, Nolan GP. Fluorescent cell barcoding in flow cytometry allows high-throughput drug screening and signaling profiling. Nat Methods. 2006; 3(5):361–368. [PubMed: 16628206]
43. Comin-Anduix B, Sazegar H, Chodon T, Matsunaga D, Jalil J, von Euw E, et al. Modulation of cell signaling networks after CTLA4 blockade in patients with metastatic melanoma. PLoS One. 2010; 5(9):e12711. [PubMed: 20856802]
44. Khan AN, Gregorie CJ, Tomasi TB. Histone deacetylase inhibitors induce TAP, LMP, Tapasin genes and MHC class I antigen presentation by melanoma cells. Cancer immunology, immunotherapy : CII. 2008; 57(5):647–654.
45. Nazarian R, Shi H, Wang Q, Kong X, Koya RC, Lee H, et al. Melanomas acquire resistance to B-RAF(V600E) inhibition by RTK or N-RAS upregulation. Nature. 2010; 468(7326):973–977. [PubMed: 21107323]

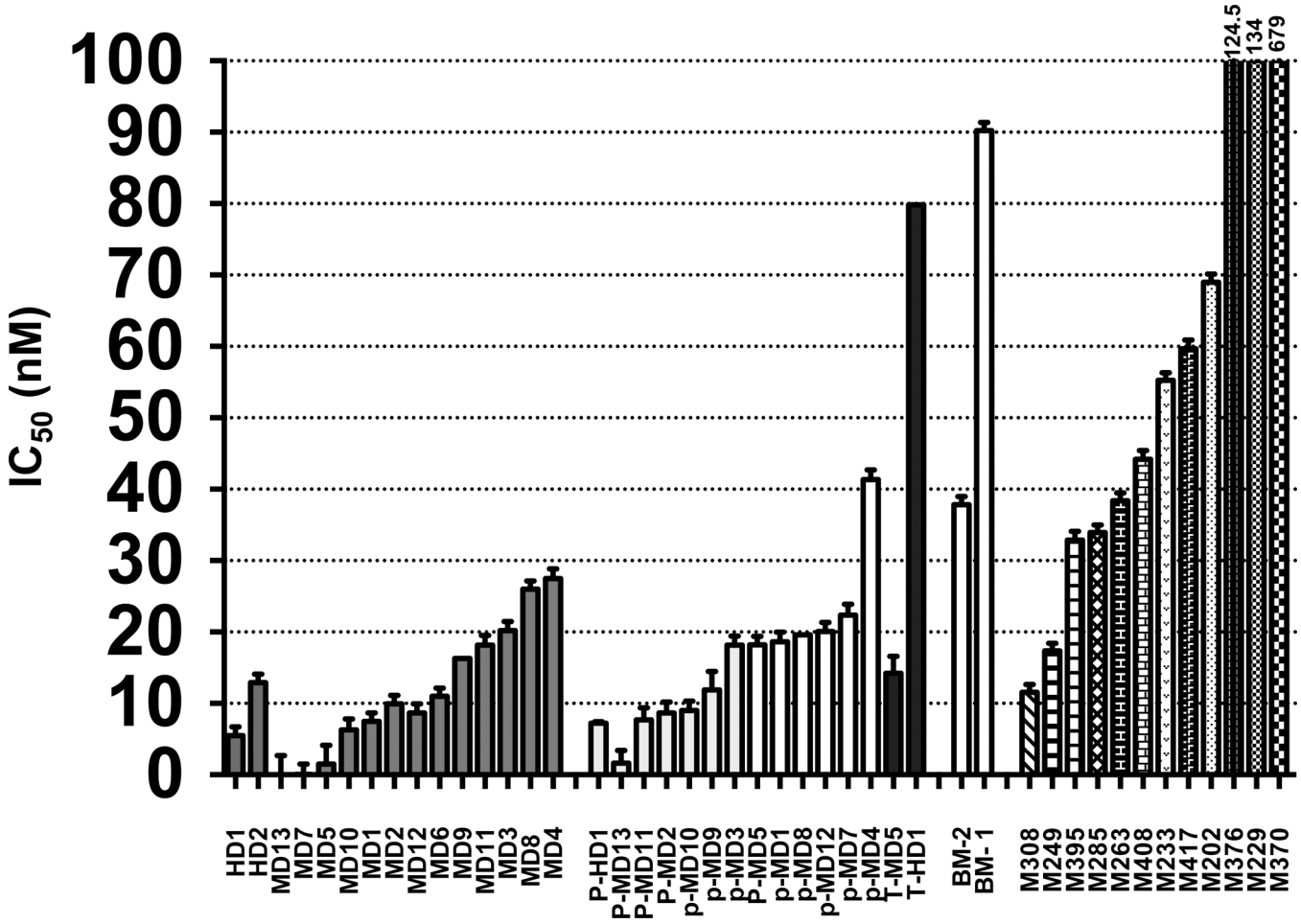

Figure 1. Panobinostat inhibits cell growth *in vitro*

Resting or proliferating (P-) PBMCs from healthy donors (HD1, HD2), from patients with metastatic melanoma (MD1, 2, 3, 4, 5, 6, 7, 8, 9, 10, 11,12, 13), PBMC from a healthy donor (HD) or from a patient with metastatic melanoma (MD) were genetically modified to express the TCR for melanoma antigen MART-1 (T-HD1), bone marrow from patients with multiple myeloma (BM1) or breast cancer (BM2), or 12 melanoma cell lines (M202, M229, M233, M249, M263, M370, M376, M285, M395, M308, M408, M417), were treated with 0–100 μM LBH589. Each data represent the mean of triplicate experiments performed 3 independent times (n=9). Bars are error bars.

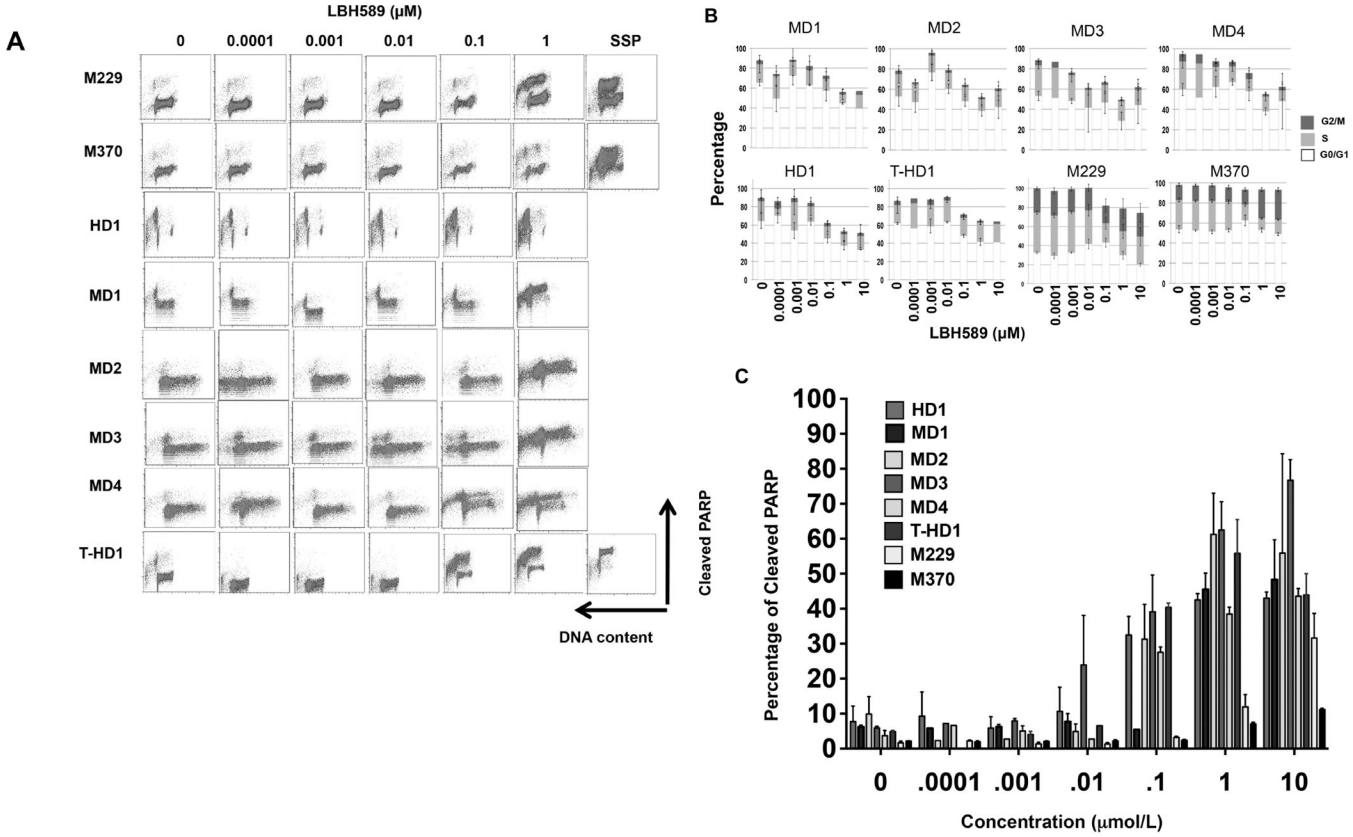

Figure 2. Effect of panobinostat on cell cycle progression and apoptosis in melanoma cell lines and activated lymphocytes

(**A**) Two melanoma cell lines (M229 and M370), PBMC cultures from a healthy donor (HD1), from patients with metastatic melanoma (MD1, 2, 3, 4), or from a healthy donor followed by genetic modification to express the TCR for melanoma antigen MART-1 (T-HD1) were treated with 0–1 μM LBH589 or 1 μM staurosporine (SSP) for 24 hours. (**B**) Quantitative analysis of the percentage of cells in G0/G1 (white), G2/M (black), or S phase (grey). (**C**) Quantitative analysis of the percentage of cells with cleaved PARP. Columns represent mean values of three independent experiments (n=3); bars, SEM.

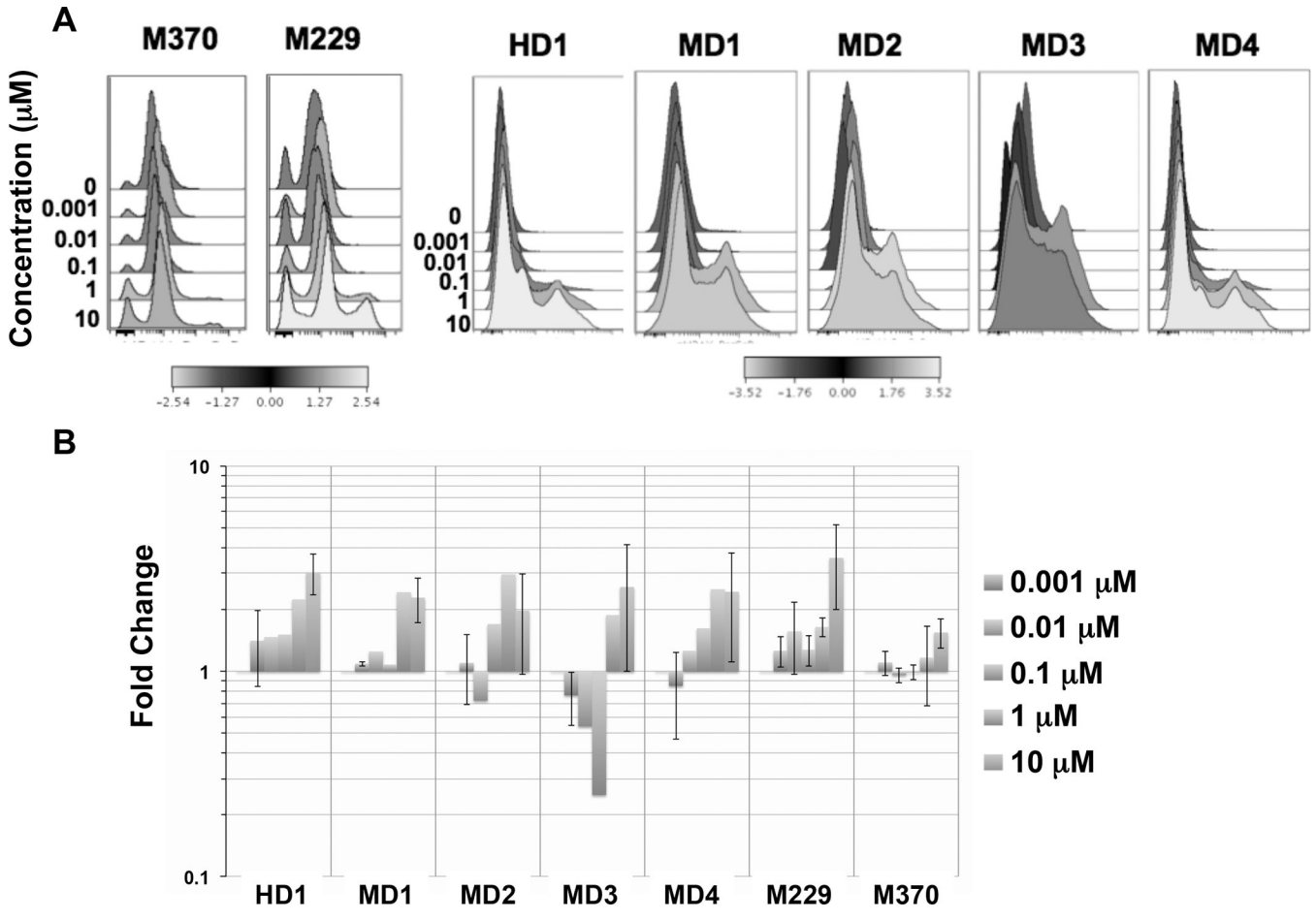

Figure 3. Panobinostat induces DNA damage in melanoma cell lines and human lymphocytes

M229 and M370, PBMC from a healthy donor (HD-1), from patients with metastatic melanoma (MD1, 2, 3, 4), or from a healthy donor followed by genetic modification to express the TCR for melanoma antigen MART-1 (T-HD1) were treated with 0–10 μM LBH589 for 24 hours, stained for pH2Ax and analyzed by flow cytometry (**A**). Colors represent fold-change with respect to the vehicle control (blue, decreased; black, no change; yellow increased). Numbers indicate magnitude of the fold-change (negative, decreased; positive, increased relative to controls) (**B**) Quantitative analysis of DNA Damage. n=3; bars are SEM.

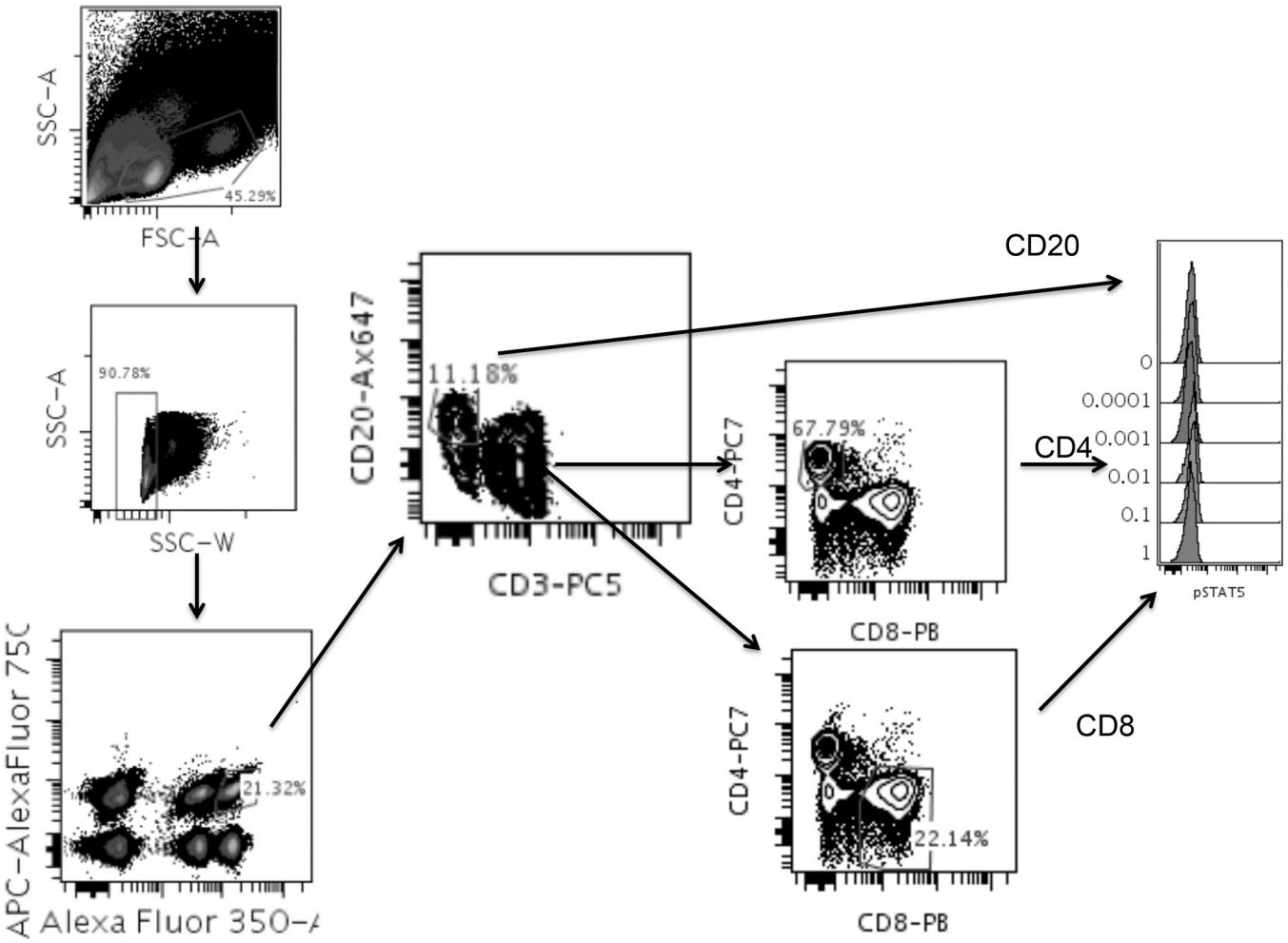

Figure 4. Single cell phosphoprotein flow cytometry gating strategy

Cells were treated with 0–1μM panobinostat for 24 hours. Cell events were first identified by gating on morphology (SSC-A vs. FSC-A) and singlets (SSC-A vs. SSC-W). After that, the six barcoded cell populations with a combination of Ax-350-NHS 0, 3, or 8 μg/mL and Ax-750-NHS 0, 3, or 8 μg/mL were deconvoluted. Then, for each of the 6 populations, plotting CD20 vs. CD3 identified B- and T-cell populations. Further plotting the CD3 population for CD4 and CD8 identified these T-cell subpopulations. Histograms of Intracellular phosphorylated proteins such as pSTAT5 were then obtained.

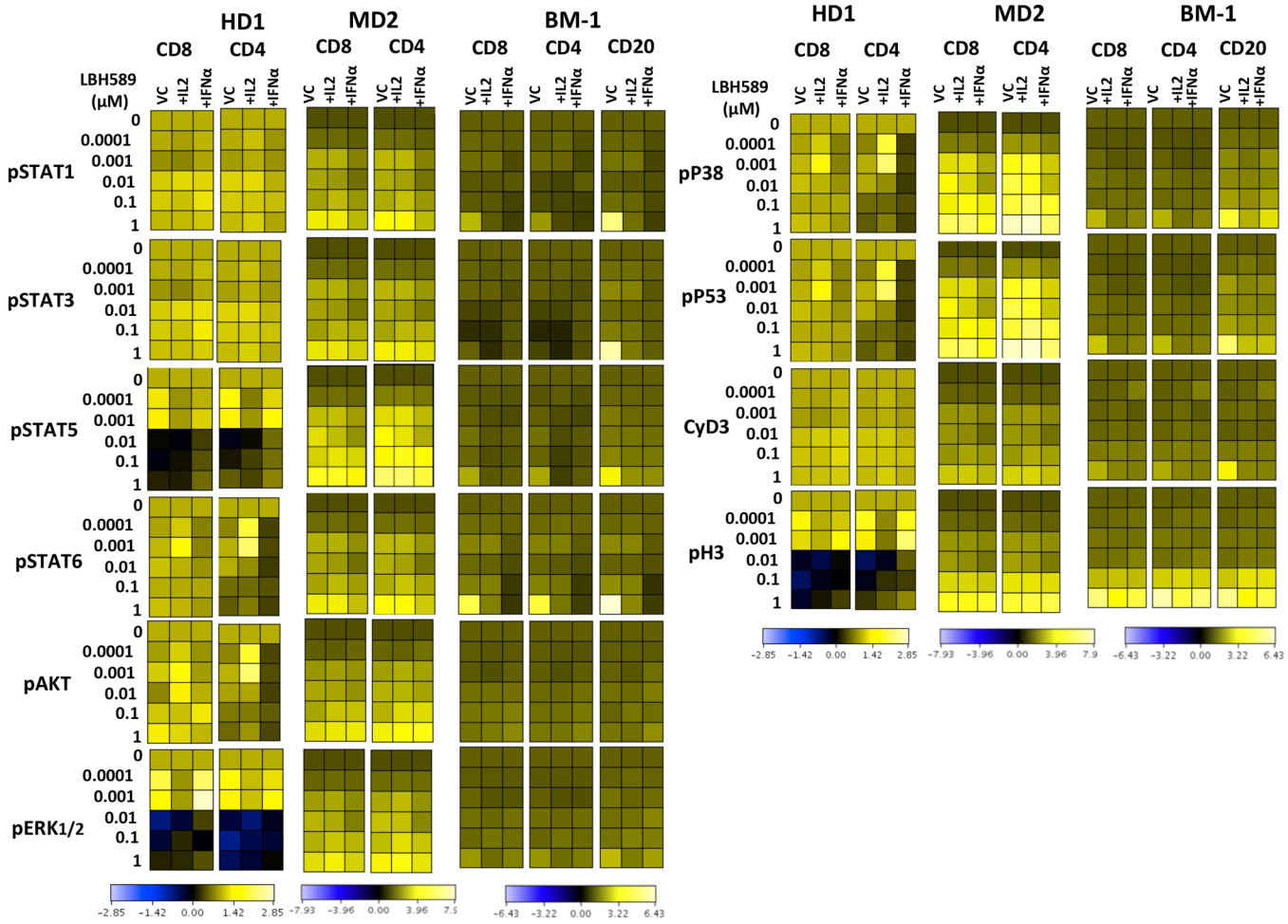

Figure 5. Quantitative analysis of the effect of panobinostat on intracellular protein phosphorylation at the single cell level

PBMC from a healthy donor (HD1), a patient with metastatic melanoma (MD), or bone marrow from a patient with multiple myeloma (BM1) were treated with 0–1μM LBH589 for 24 hours. Cells were not stimulated (vehicle control=VC) or stimulated with IL2 or IFN-α for 15 minutes, then fluorescently barcoded. $CD20^{+}CD4^{+}$ or $CD8^{+}$ cells were then evaluated for phosphorylated intracellular proteins. Results are plotted as fold-change relative to controls (blue, decreased; black, no change; yellow, increased. Values are magnitude of fold-change relative to controls).

Table 1

Characteristics of Melanoma Cell Lines

Cell Line	*BRAF* or *NRAS* Mutational Status	Other oncogenic events or tumor suppressor deletions	Sensitive (S) or Resistant (R) to Vemurafenib*
M285	Wildtype (36)		R
M229	*BRAF* V600E	MITF amplification AKT1 amplification PTEN heterozygous	S (34, 35, 45)
M233	*BRAF V600E*	*AKT1* amplification *CCND1* amplification *EGFR* amplification CDKN2A heterozygous PTEN heterozygous	R (35)
M249	*BRAF* V600E	MITF amplification AKT2 amplification PTEN homozygous	S (34, 35, 45)
M263	*BRAF* V600E	*CDKN2A* heterozygous	R (34, 35)
M308	*BRAF* V600E	*MITF* amplification *AKT2* amplification *EGFR* amplification CDKN2A homozygous	R (35)
M370	*BRAF* V600E		R (34)
M395	*BRAF* V600E		S (34, 45)
M417	*BRAF* V600E	*ABL1* E255K, Y253H EGFR P753S	R
M202	*NRAS* Q61L	*EGFR* amplification CDKN2A homozygous	R (35)
M408	*NRAS* Q61K		R
M376	*BRAF*V600E/ *NRAS* Q61K		R (34)

*Sensitive: <1μM; Resistant >1μM.